

# Homologous Series of $\text{SrCoO}_{(3n-1)/n}$ Perovskites Obtained Through $\text{Br}_2$ Oxygenation of $\text{SrCoO}_{2.5}$

Lassi Karvonen, Hisao Yamauchi, and Maarit Karppinen\*

Laboratory of Inorganic Chemistry, Department of Chemistry, Helsinki University of Technology, FI-02015 TKK, Finland

Received July 2, 2008. Revised Manuscript Received September 14, 2008

Starting from brownmillerite  $\text{SrCoO}_{2.5}$ , a series of  $\text{SrCoO}_{3-\delta}$  samples with different oxygen contents up to  $3 - \delta = 2.87$  was successfully prepared using  $\text{Br}_2$  in  $\text{CH}_3\text{CN}/\text{H}_2\text{O}$  medium as an oxidant. Six different phases, including the precursor phase, were identified depending on the oxygen content. Four of the phases have been known from earlier studies, that is,  $\text{SrCoO}_{2.50}$ ,  $\text{SrCoO}_{2.75}$ ,  $\text{SrCoO}_{2.80}$ , and  $\text{SrCoO}_{2.87}$  (the latter three obtained through electrochemical and high-pressure high-temperature oxidation techniques) representing, respectively, the  $n = 2, 4, 5$ , and  $8$  members of the  $\text{SrCoO}_{(3n-1)/n}$  homologous series, whereas signatures for the  $n = 6$  and  $7$  members were revealed here for the first time.

## Introduction

Many technologically attractive transition metal oxides possess layered crystal structures and the ability to undergo reversible (low-temperature) oxidation/reduction reactions that leave the essential parts of crystal lattice, that is, specific component layers or the entire cation sublattice, untouched. Such topotactic redox reactions typically proceed via intercalation/deintercalation of cation or anion species within a crystal lattice with either vacancy or interstitial defects. Examples include the perovskite oxides  $\text{SrCoO}_{3-\delta}$ ,<sup>1–3</sup>  $\text{SrFeO}_{3-\delta}$ ,<sup>4,5</sup> and  $\text{YBa}_2\text{Cu}_3\text{O}_{7-\delta}$ <sup>6</sup> with oxygen vacancies ordered in various ways, the  $\text{K}_2\text{NiF}_4$ -type oxide  $\text{La}_2\text{CuO}_{4+\delta}$ <sup>7</sup> with oxygen interstitials, and the layered alkali compounds  $\text{Li}_x\text{CoO}_2$ ,<sup>8,9</sup>  $\text{Na}_x\text{CoO}_2$ ,<sup>8,10</sup> and  $\text{Li}_x\text{NiO}_2$ <sup>11</sup> with cation vacancies.

Here we focus on the  $\text{SrCoO}_{3-\delta}$  system in which several (metastable) oxygen-deficient single phases of orthorhombic,<sup>1,12</sup> tetragonal,<sup>1</sup> and cubic<sup>2,3,13</sup> symmetries have been attained up to now. At  $\delta = 0.5$  the oxygen vacancies are

ordered into alternately stacked layers of corner-sharing  $\text{CoO}_4$  tetrahedra and  $\text{CoO}_6$  octahedra as in the mineral brownmillerite.<sup>12</sup> In situ characterization has revealed that room-temperature electrochemical oxygenation of  $\text{SrCoO}_{2.50}$  proceeds along a cascade of oxygen-vacancy-ordered phases, namely,  $\text{SrCoO}_{2.50}$  (orthorhombic)  $\rightarrow$   $\text{SrCoO}_{2.75}$  (cubic)  $\rightarrow$   $\text{SrCoO}_{2.75-2.89}$  (tetragonal)  $\rightarrow$   $\text{SrCoO}_{3.00}$  (cubic),<sup>3</sup> whereas Takeda et al.<sup>1</sup> obtained by means of high-pressure high-temperature synthesis a single-phase sample of  $\text{SrCoO}_{2.80}$  for which X-ray diffraction revealed some superlattice reflections presumably due to a tetragonally distorted crystal structure. The oxygen-ordered phases in  $\text{SrCoO}_{3-\delta}$  and other related perovskite systems such as  $\text{LaCoO}_{3-\delta}$ ,<sup>14</sup>  $\text{LaNiO}_{3-\delta}$ ,<sup>15</sup> and  $\text{SrFeO}_{3-\delta}$ <sup>16</sup> have been described as members of  $\text{ABO}_{(3n-1)/n}$  ( $n = 1, 2, 3, 4, \dots, \infty$ ) homologous series. In terms of stoichiometry,  $\text{SrCoO}_{2.50}$ ,  $\text{SrCoO}_{2.75}$ ,  $\text{SrCoO}_{2.80}$ , and  $\text{SrCoO}_{3.00}$  would be, respectively, the  $n = 2, 4, 5$ , and  $\infty$  members of the  $\text{SrCoO}_{(3n-1)/n}$  series. Note that for the  $\text{SrFeO}_{(3n-1)/n}$  system even the  $n = 1$  member, that is,  $\text{SrFeO}_2$ , has been realized.<sup>5,17</sup>

In the present work we selected a low-temperature chemical oxygenation route with bromine as the oxidant for the  $\text{SrCoO}_{3-\delta}$  system. The main question concerned whether it would be possible to identify some of the members of the  $\text{SrCoO}_{(3n-1)/n}$  series which have remained unattainable in studies employing other oxygenation routes, that is, electrochemical<sup>2,3</sup> and high-pressure high-temperature<sup>1,18</sup> oxygenation routes. So far alkaline hypobromite  $\text{BrO}^-$  solutions have been used as an oxidant for various Cu, Fe, and Co oxides, that

\* To whom correspondence should be addressed. E-mail: maarit.karppinen@tkk.fi.

- (1) Takeda, Y.; Kanno, R.; Takada, T.; Yamamoto, O.; Takano, M.; Bando, Y. *Z. Anorg. Allg. Chem.* **1986**, *540/541*, 259.
- (2) Nemudry, A.; Rudolf, P.; Schöllhorn, R. *Chem. Mater.* **1996**, *8*, 2232.
- (3) Le Toquin, R.; Paulus, W.; Cousson, A.; Prestipino, C.; Lamberti, C. *J. Am. Chem. Soc.* **2006**, *128*, 13161.
- (4) Nemudry, A.; Weiss, M.; Gainutdinov, I.; Boldyrev, V.; Schöllhorn, R. *Chem. Mater.* **1998**, *10*, 2403.
- (5) Tsujimoto, Y.; Tassel, C.; Hayashi, N.; Watanabe, T.; Kageyama, H.; Yoshimura, K.; Takano, M.; Ceretti, M.; Ritter, C.; Paulus, W. *Nature* **2007**, *450*, 1062.
- (6) Hinks, D. G.; Chmaissem, O.; Ely, L.; Scott, C.; Jorgensen, J. D.; Akujieze, J. K. *Physica C* **2000**, *333*, 1.
- (7) Rudolf, P.; Schöllhorn, R. *J. Chem. Soc., Chem. Commun.* **1992**, 1158.
- (8) Kikkawa, S.; Miyazaki, S.; Koizumi, M. *J. Solid State Chem.* **1986**, *62*, 35.
- (9) Motohashi, T.; Katsumata, Y.; Ono, T.; Kanno, R.; Karppinen, M.; Yamauchi, H. *Chem. Mater.* **2007**, *19*, 5063.
- (10) Karppinen, M.; Asako, I.; Motohashi, T.; Yamauchi, H. *Phys. Rev. B* **2005**, *71*, 092105.
- (11) Arai, H.; Sakurai, Y. *J. Power Sources* **1999**, *81–82*, 401.
- (12) Grenier, J. C.; Ghodbane, S.; Demazeau, G.; Pouchard, M.; Hagenmuller, P. *Mater. Res. Bull.* **1979**, *14*, 831.
- (13) Bezdzicka, P.; Wattiaux, A.; Grenier, J. C.; Pouchard, M.; Hagenmuller, P. *Z. Anorg. Allg. Chem.* **1993**, *619*, 7.

- (14) Hansteen, O. H.; Fjellvåg, H.; Hauback, B. C. *J. Mater. Chem.* **1998**, *8*, 2081.
- (15) Sayagues, M. J.; Vallet-Regi, M.; Caneiro, A.; Gonzalez-Calbet, J. M. *J. Solid State Chem.* **1994**, *110*, 295.
- (16) Hodges, J. P.; Short, S.; Jorgensen, J. D.; Xiong, X.; Dabrowski, B.; Mini, S. M.; Kimball, C. W. *J. Solid State Chem.* **2000**, *151*, 190.
- (17) Kageyama, H.; Watanabe, T.; Tsujimoto, Y.; Kitada, A.; Sumida, Y.; Kanamori, K.; Yoshimura, K.; Hayashi, N.; Muranaka, S.; Takano, M.; Ceretti, M.; Paulus, W.; Ritter, C.; André, G. *Angew. Chem., Int. Ed.* **2008**, *47*, 5740.
- (18) Kawasaki, S.; Takano, M.; Takeda, Y. *J. Solid State Chem.* **1996**, *121*, 174.

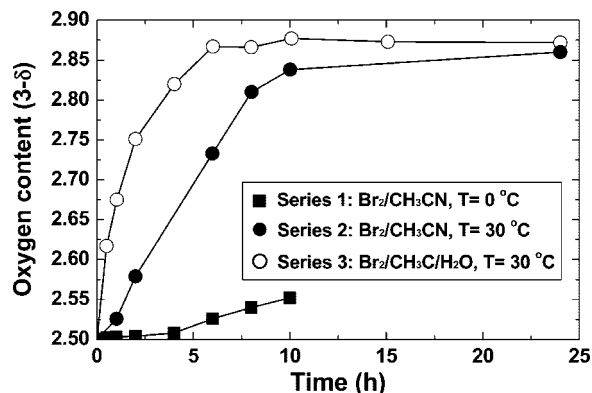


**Figure 1.** Average oxygen content per formula unit of the sample, as determined by iodometric titration, with respect to the immersion time for the three series of  $\text{SrCoO}_{3-\delta}$  samples oxygenated with  $\text{Br}_2/\text{CH}_3\text{CN}$  under different experimental conditions. Note: excluding the precursor sample and the samples with the highest oxygen contents, each sample is expected to be composed of multiple phases with different oxygen contents.

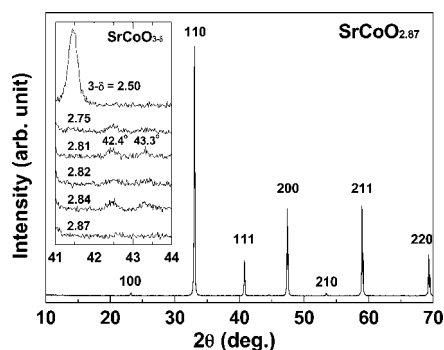


**Figure 2.** X-ray pattern of the essentially single-phase  $\text{SrCoO}_{2.87}$  sample ( $\text{Br}_2/\text{CH}_3\text{CN}/\text{H}_2\text{O}$ ,  $T = 30\text{ }^\circ\text{C}$  [Series 1], 24 h immersion). Indexation is made assuming a cubic single-perovskite unit cell. Inset: Appearance and disappearance of the superlattice reflections with increasing (average) oxygen content as demonstrated by the reflections at  $2\theta = 42.2^\circ$  and  $43.3^\circ$ .

is,  $\text{La}_2\text{CuO}_{4+\delta}$ ,<sup>7</sup>  $\text{YCuO}_{2+\delta}$ ,<sup>19</sup>  $\text{SrFeO}_{3-\delta}$ ,<sup>4</sup> and  $\text{SrCoO}_{3-\delta}$ ,<sup>2,20</sup> whereas pure bromine vapor has been used for  $\text{YBa}_2\text{Cu}_3\text{O}_{7-\delta}$ .<sup>6</sup> Here we aim at better controllability utilizing a  $\text{Br}_2$  solution diluted with acetonitrile  $\text{CH}_3\text{CN}$  (and  $\text{H}_2\text{O}$ ).

## Experimental Section

The  $\text{SrCoO}_{2.5}$  precursor used for the oxygenation experiments was prepared through an EDTA (ethylenediaminetetraacetic acid) method from stoichiometric amounts of Co and  $\text{SrCO}_3$ . Cobalt metal chunks were first dissolved in hot concentrated  $\text{HNO}_3$ , in which  $\text{SrCO}_3$  powder was added after adjusting the  $\text{HNO}_3$  concentration to 3 M. The metal nitrate solution was then poured into an equal volume of concentrated ammonia solution containing a 50% excess of EDTA against the total amount of metal ions. The solution was heated to dryness, the residual being burned and the remaining powder calcined in air at  $900\text{ }^\circ\text{C}$  for 5 h. Finally, the calcined powder was pelletized and sintered in air at  $1100\text{ }^\circ\text{C}$  for 60 h, followed by quenching to room temperature. The product was confirmed to be of the XRD-pure orthorhombic brownmillerite phase with an oxygen content of 2.50 per formula unit, as determined by iodometric titration.

Three series of  $\text{Br}_2$ -oxygenated samples were prepared by immersing 200 mg of  $\text{SrCoO}_{2.50}$  powder into 2.5 mL of 2.5 M  $\text{Br}_2/\text{CH}_3\text{CN}$  solution: within each series the immersion time was varied, but the other experimental parameters were kept fixed. The aim was to investigate the effects of temperature and  $\text{H}_2\text{O}$  addition on the oxygenation speed and the phase composition/crystal structure(s) of the oxygenated products. The experimental parameters for the three series were as follows: [Series 1]  $0\text{ }^\circ\text{C}$ , no  $\text{H}_2\text{O}$  addition, [Series 2]  $30\text{ }^\circ\text{C}$ , no  $\text{H}_2\text{O}$  addition, and [Series 3]  $30\text{ }^\circ\text{C}$ , 0.6 M  $\text{H}_2\text{O}$  addition. The oxygenation experiments were performed in  $8.5\text{ cm} \times 2.5\text{ cm}$  test tubes placed in a temperature-controlled water bath or in an ice bath and covered with a clock glass. Because  $\text{CH}_3\text{CN}$  is hygroscopic and the test tube contents were not hermetically isolated from possible sources of humidity (surrounding air and the water bath itself) it was clear that some water would be slowly accumulating in the reaction mixtures during the course of oxygenation. To see some differences between the two series, 2 (without added  $\text{H}_2\text{O}$ ) and 3 (with added  $\text{H}_2\text{O}$ ),  $\text{CH}_3\text{CN}$  solvent as water-free as possible from a freshly opened storage bottle was used. After immersion the powders were separated from the solutions, washed with acetone, and dried in hot air ( $50\text{--}90\text{ }^\circ\text{C}$ ).

The precise oxygen content was determined for each sample by means of iodometric titration:  $\sim 20\text{ mg}$  of sample powder was dry-mixed with  $\sim 3\text{ g}$  of KI and dissolved under  $\text{N}_2$  atmosphere in 30 mL of 1 M HCl solution, which was kept oxygen-free by continuous  $\text{N}_2$  bubbling. The amount of iodine produced from KI through oxidation by  $\text{Co}^{\text{III}}$  and/or  $\text{Co}^{\text{IV}}$  was immediately determined by titrating with 0.015 M  $\text{Na}_2\text{S}_2\text{O}_8$  solution using 1 mL of saturated starch solution as an indicator. Titration was repeated two to three times for each sample with reproducibility better than  $\pm 0.01$  in terms of the oxygen content,  $3 - \delta$ .

X-ray powder diffraction (XRD) patterns were recorded for all the samples by a Philips MPD 1880 diffractometer (Cu  $K\alpha$  radiation). Selected patterns were analyzed through Le Bail multiprofile matching using the software FULLPROF2000, to acquire data for the lattice parameters of the oxygenated phases. The profile of the brownmillerite phase was matched using the orthorhombic space group  $Imma$  and lattice parameters,  $a = 5.4683(3)\text{ \AA}$ ,  $b = 15.7526(7)\text{ \AA}$ , and  $c = 5.5704(2)\text{ \AA}$ , as determined for the single-phase  $\text{SrCoO}_{2.50}$  precursor sample. The profiles of the oxygenated samples were assumed to originate from several  $\text{SrCoO}_{3-\delta}$  phases with different oxygen contents. Samples with multiple oxygenated phases were matched using several overlapping profiles with unit cells all having the same cubic space group  $Pm\bar{3}m$  but different lattice parameters (plus the orthorhombic  $\text{SrCoO}_{2.50}$  phase if present). Fundamentally, for the oxygenated phases, tetragonal space groups should also be considered because of possible vacancy ordering in the oxygen sublattice.<sup>1–3</sup> However, due to the low X-ray atomic scattering factor of oxygen, peak positions in the XRD patterns for metal oxides reflect mostly the symmetry of the cation sublattice. Moreover, the oxygen-ordering-originated tetragonal distortions from the cubic symmetry in the cation sublattice are expected to be very small and nearly invisible in standard laboratory data collected using a 2-kW X-ray tube. The use of the space group  $Pm\bar{3}m$  explains, with a few exceptions mentioned below, all the reflections observed in this study.

## Results and Discussion

The present study revealed that  $\text{Br}_2/\text{CH}_3\text{CN}/\text{H}_2\text{O}$  works as an efficient oxidant for the  $\text{SrCoO}_{3-\delta}$  system. The highest oxygen content achieved was  $3 - \delta = 2.87$ , as determined by iodometric titration for samples oxygenated in  $\text{Br}_2/\text{CH}_3\text{CN}/\text{H}_2\text{O}$  at  $30\text{ }^\circ\text{C}$  for 10 h or longer. In Figure 1, oxygen contents of the samples are plotted against the immersion

(19) Trari, M.; Töpfer, J.; Doumerc, J. P.; Pouchard, M.; Ammar, A.; Hagenmüller, P. *J. Solid State Chem.* **1994**, *111*, 104.

(20) Karvonen, L.; Räsänen, S.; Yamauchi, H.; Karppinen, M. *Chem. Lett.* **2007**, *36*, 1176.

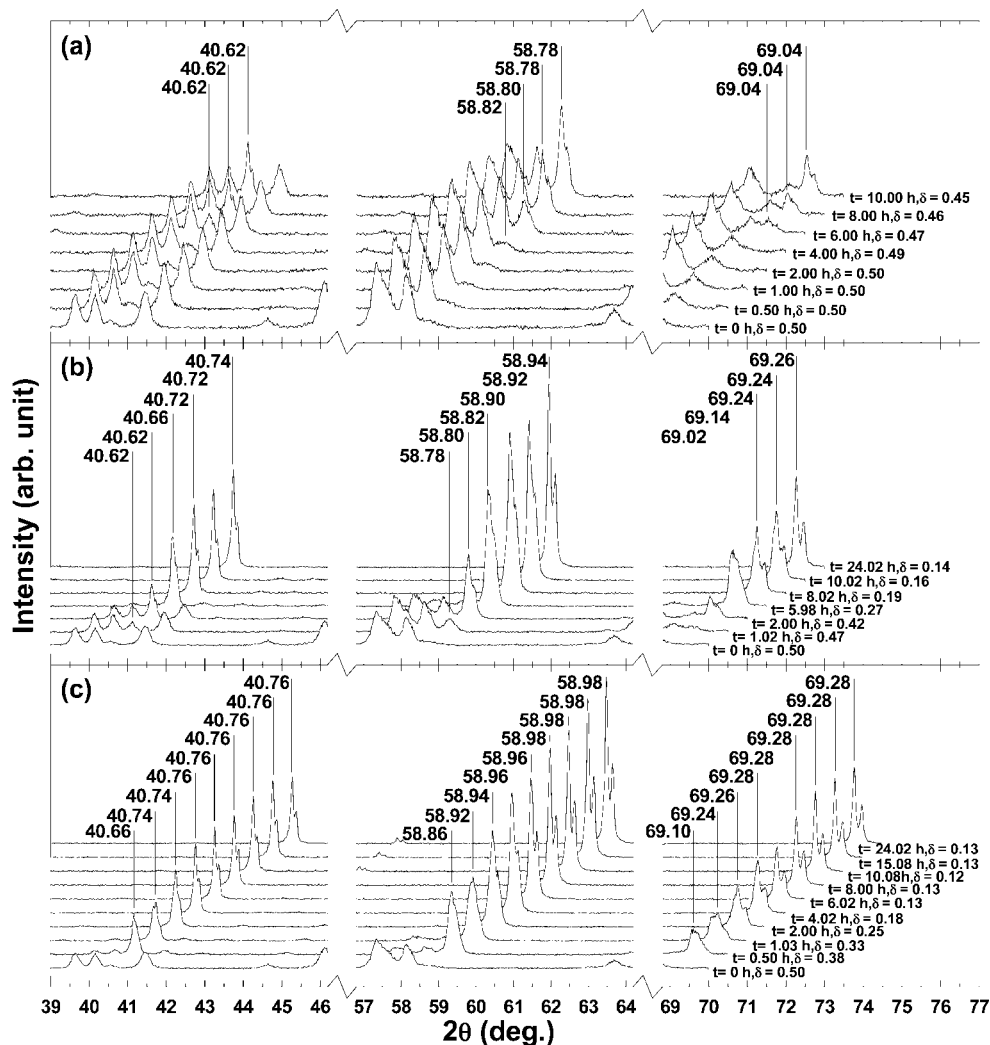


**Figure 3.** Evolution of the XRD pattern with respect to the immersion time for the three sample series: (a)  $T = 0^\circ\text{C}$ ,  $\text{Br}_2/\text{CH}_3\text{CN}$  [Series 1], (b)  $T = 30^\circ\text{C}$ ,  $\text{Br}_2/\text{CH}_3\text{CN}$  [Series 2], and (c)  $T = 30^\circ\text{C}$ ,  $\text{Br}_2/\text{CH}_3\text{CN}/\text{H}_2\text{O}$  [Series 3]. The landscape views are created by shifting the  $2\theta$  coordinates of each pattern by  $+0.5^\circ$  as compared to the coordinates of the next-lowest lying pattern, the lowest pattern in each figure having the actual  $2\theta$  coordinates of the original data set. Reflections at the  $2\theta$  values of  $40.60\text{--}40.80^\circ$ ,  $58.75\text{--}59.00^\circ$ , and  $69.00\text{--}69.30^\circ$  correspond to the indexes of (111), (211), and (220), respectively, in the cubic space group  $Pm\bar{3}m$ .

time for the three oxygenation media investigated. (Note that, as discussed below, most of the samples contain multiple  $\text{SrCoO}_{3-\delta}$  phases and the oxygen-content value obtained from iodometric titration represents a kind of average oxygen content of the sample.) From Figure 1 it is clearly seen that not only an increase in temperature but also the addition of water in the oxygenation media speed up the oxygenation process: when compared to Series 3, ( $30^\circ\text{C}$ ,  $\text{H}_2\text{O}$  added) the oxygenation rate is slightly slower if no added water was present [Series 2] and significantly slower when the mixture was cooled down to  $0^\circ\text{C}$  [Series 1].

The present observations suggest that the access of  $\text{H}_2\text{O}$  on the sample surface has a crucial role for the oxygenation to occur efficiently in the  $\text{Br}_2/\text{CH}_3\text{CN}$  immersions. Our preliminary experiments prior to this study included an immersion of  $\text{SrCoO}_{3-\delta}$  powder into pure liquid  $\text{Br}_2$  at room temperature. This approach was found not to work. Recently we reported successful oxygenation of  $\text{SrCoO}_{3-\delta}$  that had been immersed in a dispersion of  $\text{Br}_2$  and  $\text{H}_2\text{O}$ .<sup>20</sup> Compared with the sample produced in this way the oxygenation rate and the product quality are significantly enhanced in this study, where  $\text{CH}_3\text{CN}$ , readily dissolving

both the components, is used as a mixer between the otherwise mutually insoluble  $\text{Br}_2$  and  $\text{H}_2\text{O}$ . Making any conclusive statements about the reaction mechanism needs further investigations. A key reaction might, however, be the disproportionation of  $\text{Br}_2$  in  $\text{H}_2\text{O}$ , typical for all the halogens and getting less pronounced with increasing halogen atomic number. This reaction produces species of  $\text{H}^+$  and  $\text{BrO}^-$ , the latter possibly acting as the actual oxidizer. This would also be in line with the experiments by others<sup>2,4,7,19</sup> using alkaline  $\text{BrO}^-$  solutions as an oxidant for various 3d transition-metal oxide systems. Existence of acidic  $\text{H}^+$  species would further explain the total sample dissolution observed in our preliminary experiments at very high  $\text{H}_2\text{O}$  concentrations.

Judging from the XRD data, our oxygenated samples were of high quality containing only trace amounts of impurity phases ( $\text{SrCO}_3$  and  $\text{CoO}$ ), if any. At the same time most of the samples contained several different phases of  $\text{SrCoO}_{3-\delta}$ . The most strongly oxygenated samples with  $3 - \delta = 2.87$ , however, represented a single phase; see the XRD pattern in Figure 2. For some of the oxygenated samples four very weak reflections (at  $2\theta =$

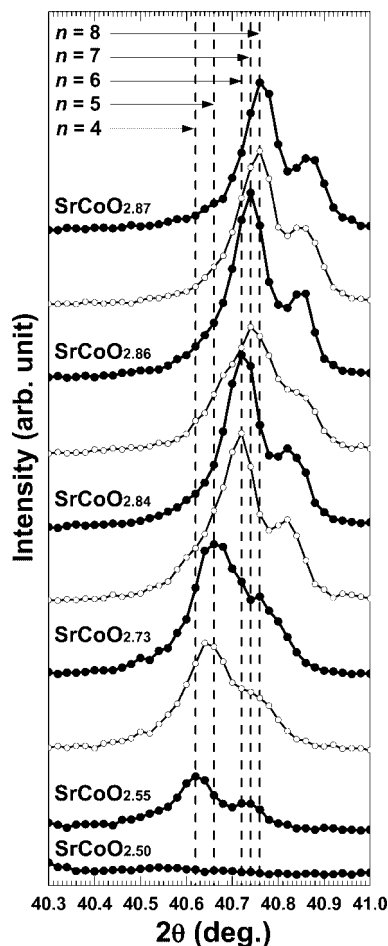


**Figure 4.** Cascade of six phases as featured by cubic (111) reflections from selected samples. Note that the oxygen contents given are average oxygen contents for samples being mixtures of several  $\text{SrCoO}_{3-\delta}$  phases (including the precursor  $\text{SrCoO}_{2.50}$  phase).

**Table 1.** Cubic Lattice Parameter  $a_c$  (e.s.d. in parentheses) for the  $\text{SrCoO}_{2.50}$  Precursor and the Five Oxygenated  $\text{SrCoO}_{3-\delta}$  Phases Detected in the Present Study<sup>a</sup>

	$a_c$ (Å)	$n$
precursor	3.914(2)	2
phase 1	3.84670(9)	4
phase 2	3.84176(7)	5
phase 3	3.83786(8)	6
phase 4	3.83635(8)	7
phase 5	3.8339(2)	8

<sup>a</sup>  $n$  refers to the index of the  $\text{SrCoO}_{(3n-1)/n}$  homologue. For the orthorhombic precursor phase,  $a_c$  was calculated as  $[(abc)/8]^{1/3}$ .

42.4°, 43.3°, 48.9°, and 65.5°) not explainable with the cubic space group  $Pm\bar{3}m$ , were observed. Takeda et al.<sup>1</sup> reported a single-phase  $\text{SrCoO}_{2.80}$  sample obtained through high-pressure high-temperature oxygenation with the same four additional reflections and interpreted them as due to tetragonal oxygen ordering. Similar superlattice reflections partly coinciding with those above were also observed in the course of electrochemical oxygenation between the stoichiometries  $\text{SrCoO}_{2.75}$  and  $\text{SrCoO}_{2.875}$  by Le Toquin et al.<sup>3</sup> In the present study the superlattice reflections (see the inset of Figure 2) were clearly detected for the  $\text{SrCoO}_{2.81}$ ,  $\text{SrCoO}_{2.82}$ , and  $\text{SrCoO}_{2.84}$  samples containing multiple  $\text{SrCoO}_{3-\delta}$  phases but not for the essentially single-phase sample of  $\text{SrCoO}_{2.87}$ .

Figure 3 displays the three most illustrative reflections of the oxygenated  $\text{SrCoO}_{3-\delta}$  phases to demonstrate the gradual changes occurring in the XRD pattern upon oxygenation for the three sample series. Moreover, Figure 4 shows the enlarged reflection at  $2\theta = 40.6\text{--}40.8^\circ$  that originates from the (111) planes in the  $Pm\bar{3}m$  cubic perovskite approach used herein. Note that this reflection remains unsplit upon tetragonal distortions. Hence, any overlapping reflections in this  $2\theta$  range would indicate the coexisting of multiple  $\text{SrCoO}_{3-\delta}$  phases with different oxygen contents. Figure 4 reveals a sequential sharpening of the (111) reflection followed by its rounding and appearance of a shoulder while it drifts toward the higher  $2\theta$  angles with increasing (average) oxygen content and decreasing (111)-plane distance. By inspecting this sequential progress in the shape of the reflection, a cascade of four intermediate phases may be distinguished on the way from  $\text{SrCoO}_{2.50}$  to the end phase,  $\text{SrCoO}_{2.87}$ . The difference in the cubic lattice parameter  $a_c$  between two subsequent oxygenated phases is as little as  $2\text{--}5 \times 10^{-3}$  Å (see Table 1). The number of the phases observed here actually fits well with the concept of homologous series,  $\text{SrCoO}_{(3n-1)/n}$ . In terms of this series, our final essentially single-phase oxygenation product of  $\text{SrCoO}_{2.87}$  is most likely to represent the  $n = 8$  homologue. Since the existence of a two-phase region between the phases,  $\text{SrCoO}_{2.50}$  and  $\text{SrCoO}_{2.75}$ , is realistic on the basis of the previous electrochemical experiments,<sup>2,3</sup> it is reasonable to assume our least-oxygenated phase to be  $\text{SrCoO}_{2.75}$ , which is the  $n = 4$  homologue in the  $\text{SrCoO}_{(3n-1)/n}$  series. Between the  $n = 4$  and 8 homologues there is room for three other homologues, which is the number of the remaining phases observed in this study. One of these phases is likely to be the  $\text{SrCoO}_{2.80}$  ( $n = 5$ ) phase obtained by Takeda et al.<sup>1</sup> by means of high-pressure high-temperature synthesis. The remaining two phases are identified here for the first time, and their number fills the gap of missing homologues with  $n = 6$  and 7. Here we should mention that even though the peak broadening and shoulder formation seen in Figure 4 could possibly be explained by orthorhombic distortions, for example, our simulation in space group  $Immm$  indicates a visible shouldering down to  $\pm 0.1\%$  difference between the  $a$  and  $b$  lattice parameters (when the dimensions of the original unit cell relate  $a = b \neq c$ ), this most likely is not the case as no signatures of orthorhombicity have been reported for any of the previously known  $\text{SrCoO}_{3-\delta}$  phases except for the  $\text{SrCoO}_{2.0}$  brownmillerite.<sup>1-3</sup>

According to previous studies and our observations as well, the  $n = 4$  and 8 phases appear to be more stable than the homologues between them. This might be due to the more isotropic distribution of oxygen vacancies available for them. To demonstrate this, we assume an ideal cubic perovskite structure: at  $n = 4$  all the oxygen vacancies may be distributed on the (002) Sr–O planes so that they form a primitive square lattice with a stoichiometry of  $\text{Sr}_4\text{O}_3/\text{vacancy}$ . If the planes are further stacked in such a way that each vacancy lies in the center of a cube cornered by 8 vacancies, 4 in the Sr–O plane above and 4 in the plane below, we obtain a bcc unit cell of vacancies with dimensions  $2a_c \times 2a_c \times 2a_c$ . Moving up to the  $n = 8$  homologue may



then be imagined step-by-stepwise through shifting every other plane of the  $n = 4$  structure by  $\sqrt{2}a_c$  along [110] for columns of vacancies to form along [001]. Filling every other vacancy column in a checker-board manner and shifting every other plane further by  $2a_c$  along [100] creates a vacancy distribution having a body-centered-tetragonal unit cell of vacancies with dimensions  $2\sqrt{2}a_c \times 2\sqrt{2}a_c \times 2a_c$ . When these vacancy structures are considered as part of the ideal cubic perovskite lattice, the possible superlattice symmetry would be  $I4/mmm$  with unit cell dimensions  $2a_c \times 2a_c \times 2a_c$  for the  $n = 4$  homologue and  $2\sqrt{2}a_c \times 2\sqrt{2}a_c \times 2a_c$  for the  $n = 8$  homologue (as described in the latter case by Hodges et al.<sup>16</sup> for  $\text{SrFeO}_{2.875}$ ). Such isotropic vacancy distributions as those for the  $n = 4$  and  $n = 8$  homologues might not be possible for the  $n = 5, 6, 7$  homologues, which explains their lower stability. Finally, we should mention here that Le Toquin et al.<sup>3</sup> have demonstrated that the low-temperature oxygenation intercalation occurs in the  $\text{SrCoO}_{3-\delta}$  system through topotactic reactions. The present results are in line with this.

We summarize our observations by comparing the appearance of each intermediate phase in the XRD patterns of Figure 3a–c. In Series 3 (Figure 3c), having added water in the oxygenation medium, the oxygenation proceeds fast (within 8 h) up to the final  $\text{SrCoO}_{2.87}$  phase leaving all the intermediate phases quite unpronounced. Series 2 with no intentionally added water (Figure 3b) leaves the different homologues to appear for several hours, slightly more separated from each other. Although the oxygenated-phase formation has just started by the end of the observations in Series 1, with no water added and moreover the oxygenation media kept at a lower temperature (Figure 3a), the reflections of the emerging least-oxygenated phase are slightly sharper

after a 10-h oxygenation than the corresponding ones after a 2-h oxygenation in Series 2. Thus, the combination of water elimination and cooling creates a better phase separation between the intermediate phases. With even more delicate adjustment of the process conditions in future studies, chances remain for us to be able to isolate the different intermediate phases for precise phase-specific oxygen-content determination and accurate crystal-structure analysis.

### Conclusion

The present study has demonstrated that bromine works as an efficient but delicate oxidant for the  $\text{SrCoO}_{3-\delta}$  system. Six different oxygen-vacancy-ordered phases including the precursor phase were distinguished as the oxygenation proceeded from  $3 - \delta = 2.50$  for the precursor phase up to the highest oxygen content of  $3 - \delta = 2.87$  achieved here. The essentially single-phase sample with  $3 - \delta = 2.87$  should be mainly composed of the  $n = 8$  member of the  $\text{SrCoO}_{(3n-1)/n}$  homologous series (with  $3 - \delta = 2.875$ ). Four out of the six phases have appeared in earlier studies, namely,  $\text{SrCoO}_{2.5}$  (orthorhombic),  $\text{SrCoO}_{2.75}$  (cubic),  $\text{SrCoO}_{2.80}$  (tetragonal), and  $\text{SrCoO}_{2.87}$  (tetragonal) representing the  $n = 2, 4, 5$ , and  $8$  members of the homologous series, respectively. Two new phases, tentatively assigned to the missing  $n = 6$  and  $7$  members, might hence have been detected here for the first time. Our findings moreover underline the usefulness of developing alternative oxygenation routes for  $\text{SrCoO}_{3-\delta}$  and related nonstoichiometric oxide systems.

**Acknowledgment.** The present work was supported by Tekes (No. 1726/31/07), Academy of Finland (No. 110433), and Finnish Foundation for Technology Promotion.

CM801761P